Electronics and Electrical Engineering

AIMS Electronics and Electrical Engineering, 7(2): 171–186.
DOI: 10.3934/electreng.2023010
Received: 24 February 2023
Revised: 06 April 2023
Accepted: 19 April 2023
Published: 22 May 2023

http://www.aimspress.com/journal/ElectrEng

Research article

Analysis of a low-profile, dual band patch antenna for wireless applications

M. Naveen Kumar[1,2], M. Venkata Narayana[2], Govardhani Immadi[2,*], P. Satyanarayana[2] and Ambati Navya[2]

[1] Department of ECE, PSCMR College of Engineering and Technology, Vijayawada, India
[2] Department of ECE, KLEF, Vaddeswaram, Guntur, Andhra Pradesh, India

*** Correspondence:** Email: govardhanee_ec@kluniversity.in**.**

Abstract: A dual-band google lens logo-based patch antenna with defected ground structure was designed at 5.3 GHz for wireless applications and 7.4 GHz for wi-fi application. The designed antenna consists of a rounded rectangular patch antenna with a partial ground structure fed by a 50 Ω microstrip line. A google lens shaped logo is subtracted from the rounded rectangular patch and some regular polygon shaped slots are subtracted from the ground plane to obtain good dual-band characteristics and better results in terms of gain, VSWR, and return loss. The proposed antenna has a measurement of 20 × 20 × 1.6 mm^3 and provides wide impedance bandwidths of 0.23 GHz (5.17–5.40 GHz) and 0.16 GHz (7.33–7.49 GHz) at center frequencies of 5.3 GHz and 7.4 GHz, respectively. The antenna was designed and simulated using an ANSYS Electronics Desktop. Fabrication of the antenna was obtained using chemical etching and the results were measured by using an MS2037C Anritsu combinational analyzer. The return loss characteristics for dual bands are -20.56 dB at 5.3 GHz and -19.17 dB at 7.4 GHz, respectively, with a VSWR < 2 at both the frequencies and a 4 dB gain is obtained.

Keywords: dual band; return loss; impedance bandwidth; VSWR; surface current distribution; radiation pattern; gain

1. Introduction

Microstrip patch antennas are popular because of their low profile, versatile nature, robustness,

ease of fabrication, affordable cost, conformal and planar structures, and many other advantages when compared to conventional antennas. These are widely used for communication within short ranges and high frequency applications. A low-profile antenna has a shorter height, width, and can be mounted on any flat surface. However, these patch antennas suffer from the drawbacks of a limited bandwidth, low directivity, and poor gain, constraining its applications. For a microstrip patch antenna, the size of the patch increases as the resonant frequency decreases; the shorter the frequency and the higher the wavelength, the larger the antenna can be made. Defected ground structure (DGS) is a novel approach with numerous applications in various fields that can be utilized in antenna design to improve antenna performance. Unlike conventional antennas, microstrip patch antennas are famous for their simple and compact structures, small size, and can be installed on any conformal plane within small area. They also exhibit good radiation characteristics with a considerable gain and directivity [1]. DGS is a technique that helps us improve characteristics such as increasing the bandwidth and the resonant frequency [2]. DGS also leads to miniaturization of the antenna and enhances the bandwidth [3]. Putting slots on the patch, using DGS, and altering the feed position will also contribute to obtaining circular polarization, which helps in impedance matching and improvement of return loss [4]. A microstrip patch antenna array with FR-4 epoxy as the substrate for C-band application is shown in [5], where the size of the antenna is large for C-band 80 x 80 mm^2 applications and dual band response is achieved with high gain, which can be used as a receiving antenna for distance transmission. This antenna array is designed by modifying the initially designed single element patch antenna. This paper [6] shows how an antenna array with two elements of a maple-leaf shape containing three slots across the diagonal is designed for the C-band with an operating frequency of 7.45 GHz and is circularly polarized. A tri-band antenna with gap-coupled parasitic patches around the circular radiating patch results in three resonant frequencies, as shown in [7]. A parasitic patch antenna of an L shape which operates at three modes is proposed in [8], with an impedance bandwidth at all three frequencies. In [9], a multi-layered patch antenna is proposed with an aperture coupling for mutual coupling reduction between the array elements where two substrates are used, and the radiating element is placed on top of the upper substrate and the feeding is given from the bottom. However, the use of a multi-layered substrate makes the design complex than a simple patch antenna. A wideband 4 × 4 antenna array with stacked microstrip is proposed in [10], which uses a substrate integrated waveguide for feeding. These stacked microstrips are more complex while designing as integration of layers is needed but has good radiation efficiency. MIMO antennas are one of the key technologies with high efficiency and an accuracy in the field of wireless communications with large number of applications. A triple-band, two-port, MIMO antenna is shown in [11], which used stub geometry for C-band applications. Chen et al. [12] shows a design of an eight-port patch antenna for a C-band with a MIMO system which is both larger thicker. Electromagnetic band-gap structures are widely used to enhance the performance of the antenna, especially for the reduction of mutual coupling in the MIMO antennas. These band gap structures are sometimes placed between the array elements as either stubs or in the shape of some creative structures, as demonstrated in [13,14]. Monopole microstrip patch antennas usually consist of either partial or semi-infinite ground structures and are mostly bi-directional [15]. A monopole patch antenna structure is shown in [16–21], with an enhanced gain by using the two monopole elements.

In all the above analyses, these antennas either had complex structures with large areas or did not cover the frequency bands of wireless applications at 5.3 GHz and 7.4 GHz. This work presents the design of a dual band, google lens, microstrip patch antenna with some regular polygon shaped

slots in the ground plane for wireless applications. Wide impedance bandwidths of 0.23 GHz (5.17–5.40 GHz) and 0.16 GHz (7.33–7.49 GHz) at center frequencies of 5.3 GHz and 7.4 GHz were utilized for wireless applications and WIFI applications, respectively. The return loss characteristics for dual bands are -20.56 dB at 5.3 GHz and -19.17 dB at 7.4 GHz, respectively, with a VSWR < 2 at both the frequencies and a 4 dB gain is obtained. This antenna achieves a considerable peak gain of 4 dB with a radiation efficiency of 61.7% at both resonant frequencies. Moreover, the proposed antenna offers an omnidirectional radiation pattern in both the E and H-planes. The work is categorized as follows: Part 1 contains an introduction and a literature review. Part 2 contains a detailed overview of the design. Part 3 explains the results and part 4 wraps up the proposed work.

2. Antenna design and configuration

First, the proposed dual-band patch antenna is based on designing a rectangular patch antenna using basic microstrip patch antenna design considerations and then altering the antenna geometry to reach the desired dual band resonant frequencies. A rectangular patch antenna only has a good return loss in a particular frequency range. To attain dual band characteristics, this basic patch antenna design underwent a few changes. A FR4 epoxy material with a height of 1.6 mm was employed as the substrate [22–26].

The proposed antenna has a size of 20 × 20 mm^2 and is fed with a 50 Ω microstrip transmission line. The width of the rounded rectangular radiating patch is 18 mm and the length is 12 mm, which is center fed by a feed line with a length of 9 mm and a width of 1 mm. A google lens logo slot of size 6 mm × 6 mm is removed from the rounded rectangular patch. Initially, the ground plane's width is 20 mm and the length is 20 mm. Later, the size of the ground is partially reduced and modified by removing some regular polygon shapes and a circle in the middle of the ground plane. Figure 1 shows a rounded rectangular patch without DGS. Figure 1 represents the basic microstrip patch antenna, Figure 2 represents the google lens logo antenna with full ground, and Figure 3 represents the google lens antenna with a partial ground having triangular slots.

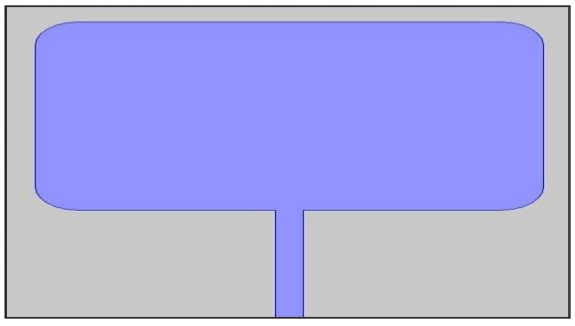

Figure 1. Iteration-1.

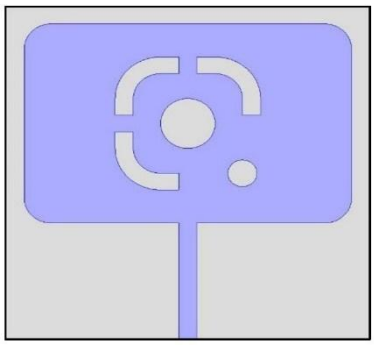

Figure 2. Iteration-2.

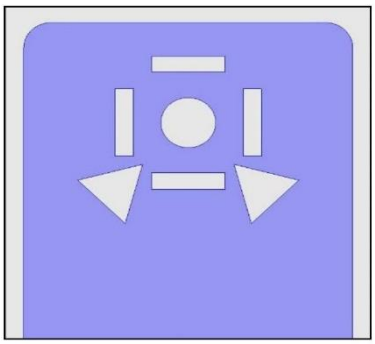

Figure 3. Iteration-3.

A basic microstrip patch antenna is designed and resonates at 5.3 GHz and 7.4 GHz, with a minimal amount of return loss at both the frequencies. In the second iteration, a google lens logo shape is subtracted from the basic antenna to obtain an improved amount of return loss; at this point, an improved return loss has been obtained at both the frequencies and, at last, we have subtracted a polygon type structure from the ground. After subtracting that portion from the ground plane, a very minimal amount of return loss was obtained at both the frequencies with a return loss of -15 dB at 5.3 GHz and -22 dB at 7.4 GHz for wireless communication applications. Figure 4 represents the top and bottom views of the microstrip rounded rectangular patch antenna. The dimensions that are utilized while designing the antenna are represented in Table 1. Figure 5 represents the fabricated prototype of the designed antenna in both top and bottom views.

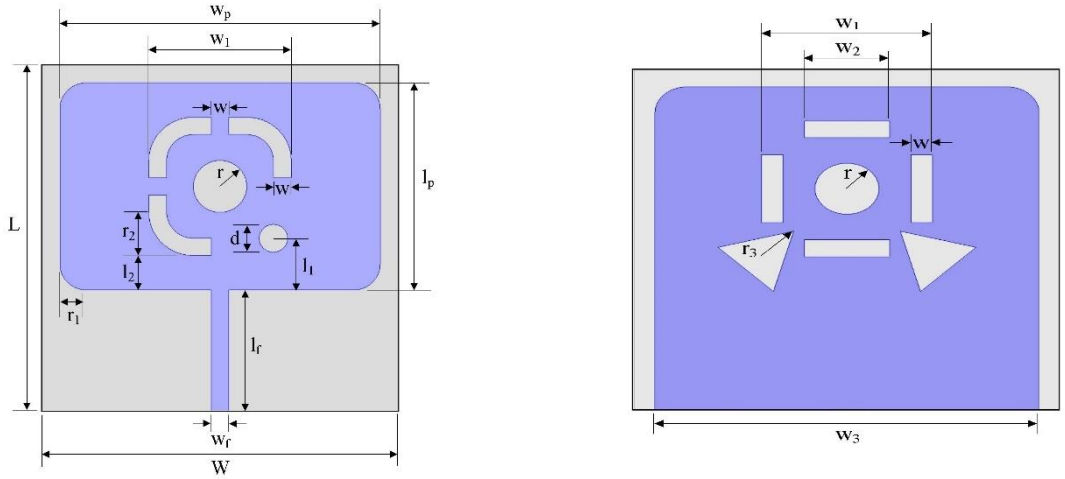

(a) (b)

Figure 4. Proposed antenna (a) Top view and (b) Bottom view.

Table 1. Design parameters values of the antenna.

Parameters	Dimensions (mm)	Parameters	Dimensions (mm)
W	20	l_f	7
w_p	18	l_1	3
w_f	1	l_2	2
w_1	8	d	1.6
w_2	4	r	1.5
w	1	r_1	1.5
L	20	r_2	2.5
l_p	12	r_3	1.5

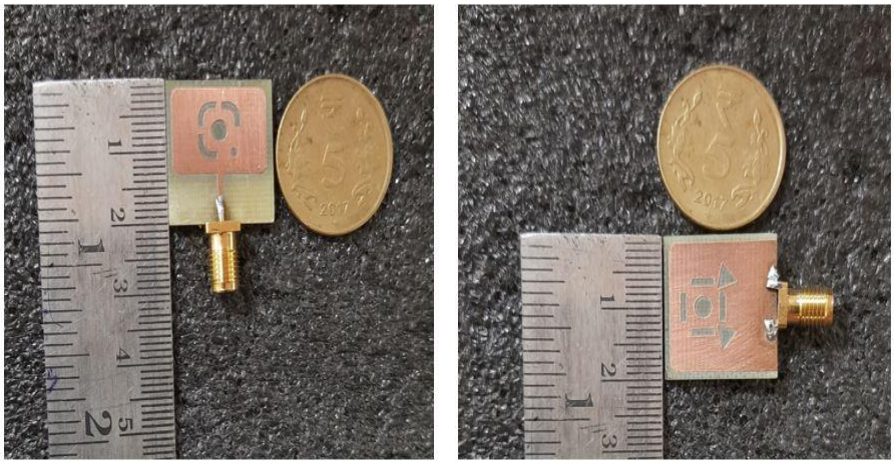

(a) (b)

Figure 5. Photograph of fabricated antenna (a) Top view and (b) Bottom view.

3. Results

The simulation of the suggested antenna was carried out in an Ansys Electronic Desktop, which is based on the finite element method, and the HFSS-IE uses the method of moments (MoM) [27–30]. The antenna was excited by a lumped port and the boundary box had an area of 100 mm × 100 mm × 50 mm [31,32]. Parametric studies for the step wise antenna design are represented in Figure 7. To prove that the simulation results are accurate, the suggested antenna was manufactured as depicted in Figure 5. Figure 6 represents the return loss of the rounded rectangular microstrip patch antenna having triangular shaped slots in the ground plane. The blue color line indicates the return loss of the first antenna iteration, where the return loss obtained is -10 dB at 5.3 GHz and -13 dB at 7.4 GHz. The black color dotted line represents the return loss of the second antenna iteration, where the return loss obtained is -12 dB at 5.3 GHz and -17 dB at 7.4 GHz. The red color solid line represents the return loss of the final antenna iteration, where the return loss obtained is -15 dB at 5.3 GHz and -20.2 dB at 7.4 GHz, which is suitable for wireless communication applications. The reflection coefficient S_{11} was measured using a MS2037C combinational analyzer. The variation of the reflection coefficient S_{11} of the suggested antenna is illustrated in Figure 7. The measured results shows that the antenna presents a broadband of 0.23 GHz (5.17–5.40 GHz) and 0.16 GHz (7.33–7.49

GHz) with two resonant frequencies at 5.3 and 7.4 GHz with reflection coefficients of -15 dB and -20.5 dB, respectively. Chemical etching has been used for the design of the antenna. A return loss of -12 dB at 5.3 GHz and -18 dB at 7.4 GHz has been obtained for the measured antenna. Figure 9 depicts the simulated surface current distribution of the suggested broadband antenna results acquired by an Ansys Electronic desktop at resonant frequencies 5.3 and 7.4 GHz. The measured return loss of the antenna is obtained by connecting the antenna to the combinational analyzer and the radiation pattern of the antenna is obtained by using an anechoic chamber by connecting the proposed antenna to the receiver end and the source antenna is taken as the standard horn antenna for measurement.

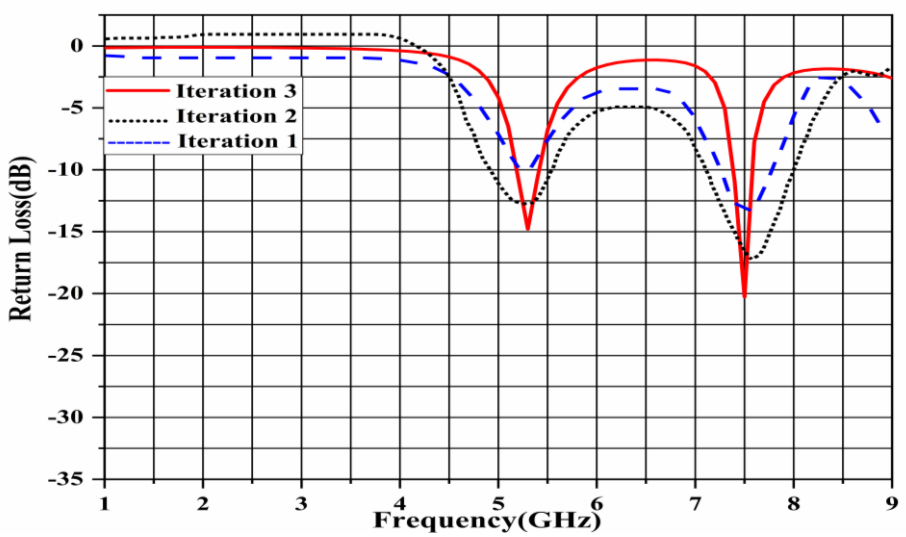

Figure 6. Return loss plot of the designed antenna for all iterations.

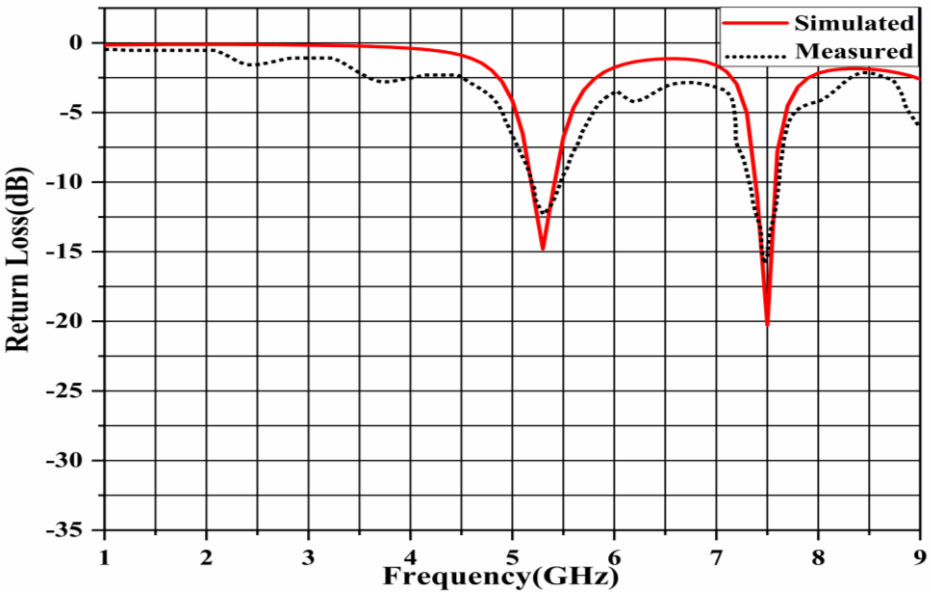

Figure 7. Simulated & Measured return loss plot of the proposed antenna.

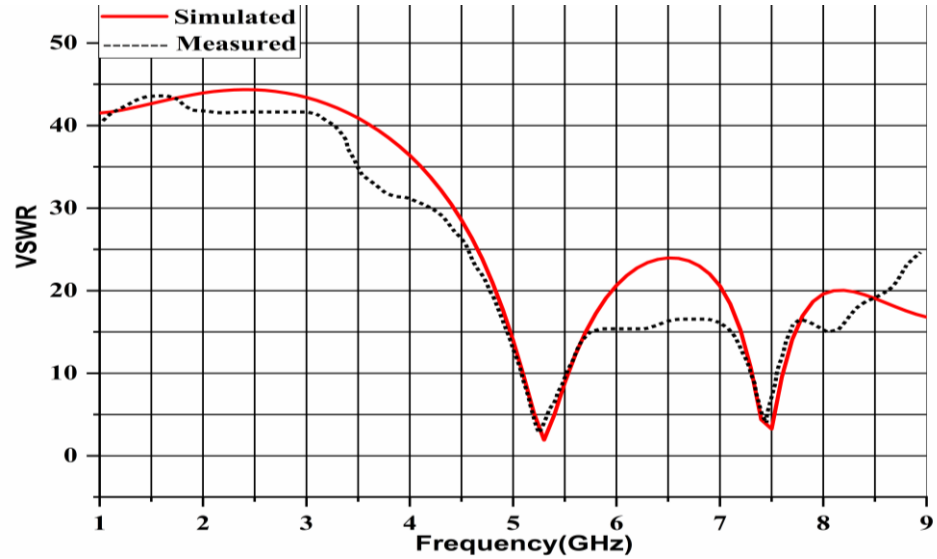

Figure 8. VSWR plot of the proposed antenna.

The proposed antenna is reported to have a high radiation pattern performance in the figure because it achieves an omnidirectional pattern in both the H-plane and the E-plane. The suggested antenna's radiation pattern and peak gain were measured in an anechoic room, as seen in Figure 10. Additionally, Figure 10 shows the observed radiation pattern at resonant frequencies of 5.3 and 7.4 GHz along with the simulated outcomes obtained by the Ansys simulated antenna and the manufactured antenna. The recommended antenna is reported to have ahigh radiation pattern performance in the figure because it achieves an omnidirectional pattern in both the H-plane and the E-plane. Figure 11 shows the observed peak gain at both resonating frequencies. It is clear from the numbers that the recommended aerial performs well in terms of peak gain and radiation efficiency. At both resonant frequencies, the aerial provides a sizable gain of 4.029 dB. The VSWR of the antenna is shown in Figure 8, with a value less than 2 at both frequencies, which are 1.20 at 5.3 GHz and 1.24 at 7.4 GHz. The surface current distributions at the dual-band are shown in Figure 9, where the maximum current density is 189 Am^{-1} and 173 Am^{-1} at 5.3 GHz and 7.4 GHz, respectively, which is due to the coupling between feed line and patch. The maximum current density of the rounded rectangular patch without slots and DGS is 50 Am^{-1} and 49 Am^{-1}, respectively, from which we can observe that the current density increases after altering the structure by putting slots and using defected ground. It is seen that the path of the current distribution is different for the two frequencies and is three times more than that of the antenna model with slots rather than the antenna model without slots. At a resonance of 5.3 GHz, the current is distributed vertically, whereas at a resonance of 7.4 GHz, the current is distributed horizontally. Figures 10–13 represent the radiation pattern of the proposed antenna by varying the elevation and azimuthal angles at two resonating frequencies. It can be observed that the cross-polarization is very low at 5.3 GHz in both the E-plane and H-plane. Figure 14 represents the gain of the proposed antenna and a gain of 4 dB is obtained at both frequencies.

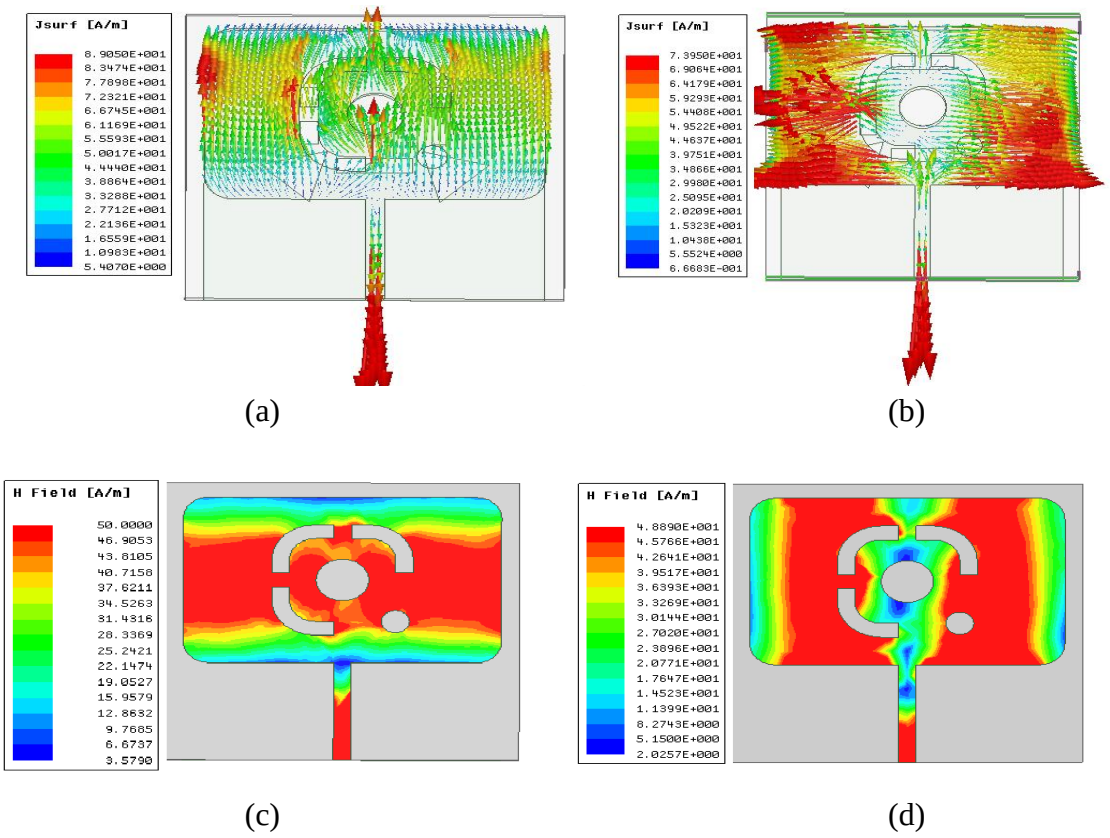

Figure 9. (a) Vector current distribution at 5.3 GHz (b) Vector current distribution at 7.4 GHz (c) H-Field of the proposed antenna at 5.3 GHz (d) H-Field of the proposed antenna at 7.4 GHz.

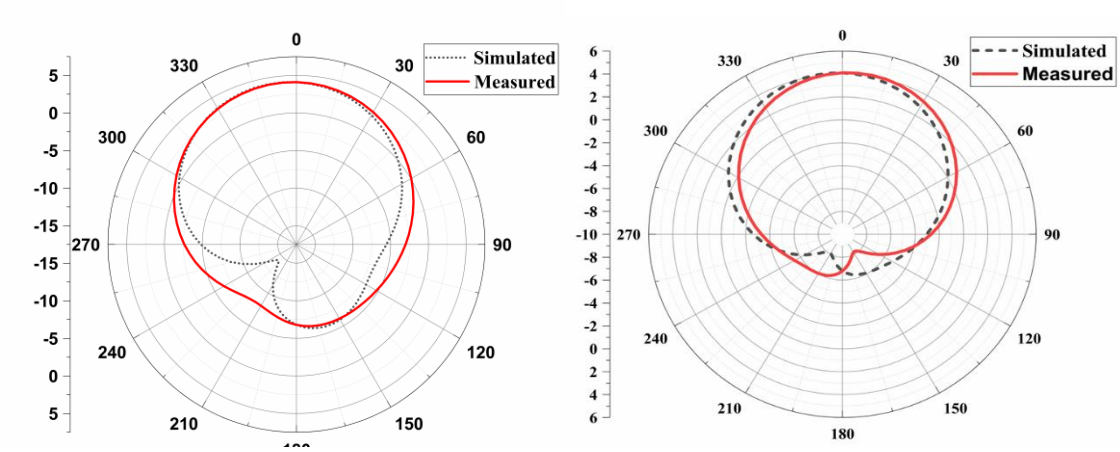

Figure 10. Simulated and measured radiation pattern of the proposed antenna in terms of azimuthal angle at 5.3 GHz (a) $\Phi = 60^{o}$ (b) $\Phi = 120^{o}$ (c) $\Phi = 180^{o}$.

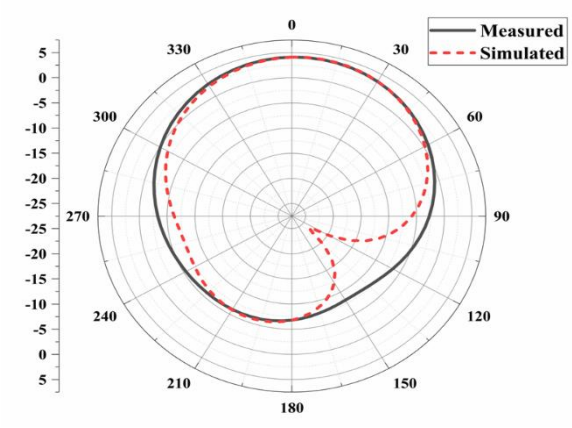

(c)

Figure 10. Continued.

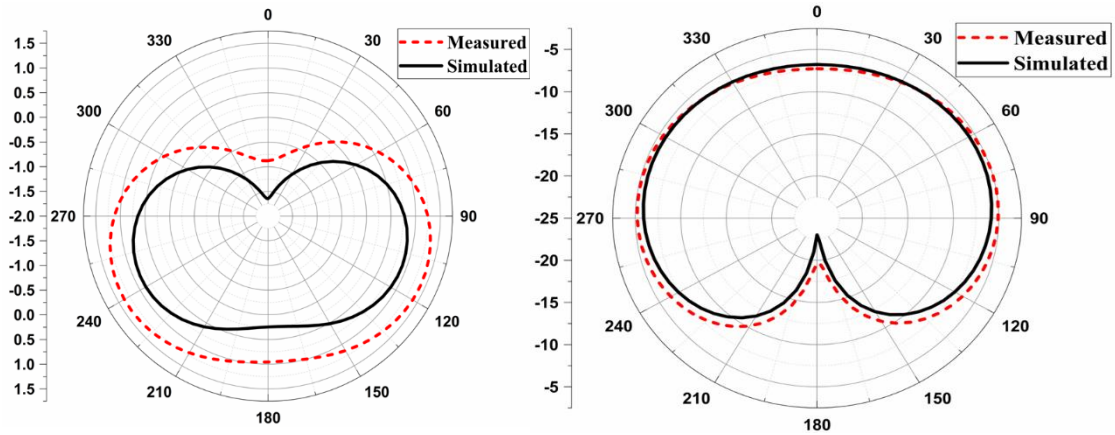

(a) (b)

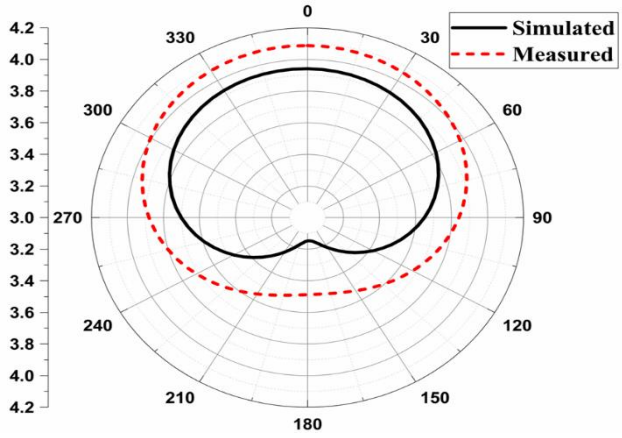

(c)

Figure 11. Simulated and measured radiation pattern of the proposed antenna in terms of azimuthal angle at 7.4 GHz (a) $\Phi = 60^{o}$ (b) $\Phi = 120^{o}$ (c) $\Phi = 180^{o}$.

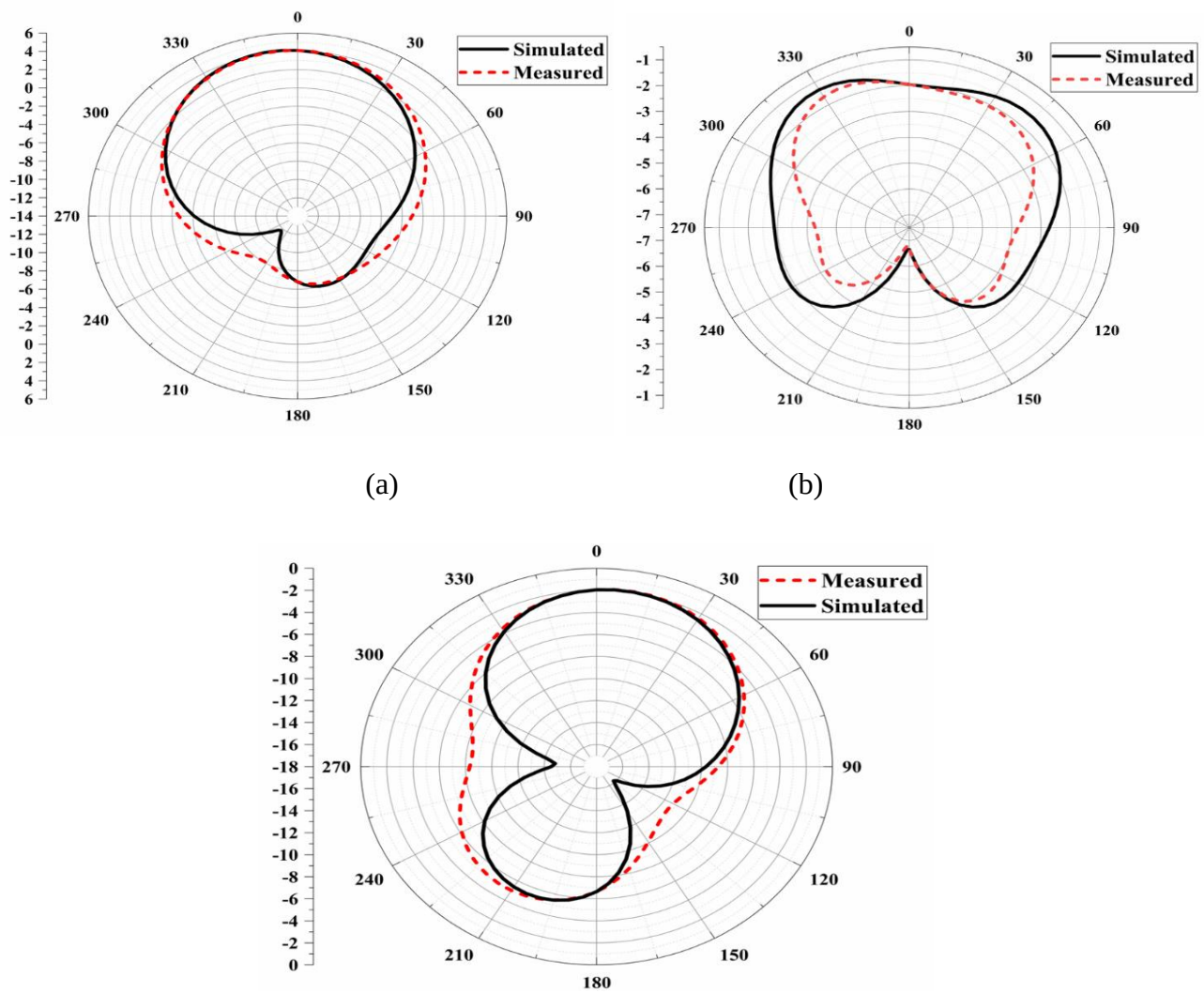

Figure 12. Simulated and measured radiation pattern of a proposed antenna in terms of elevation angle at 5.3 GHz (a) $\theta = 60^{o}$ (b) $\theta = 120^{o}$ (c) $\theta = 180^{o}$.

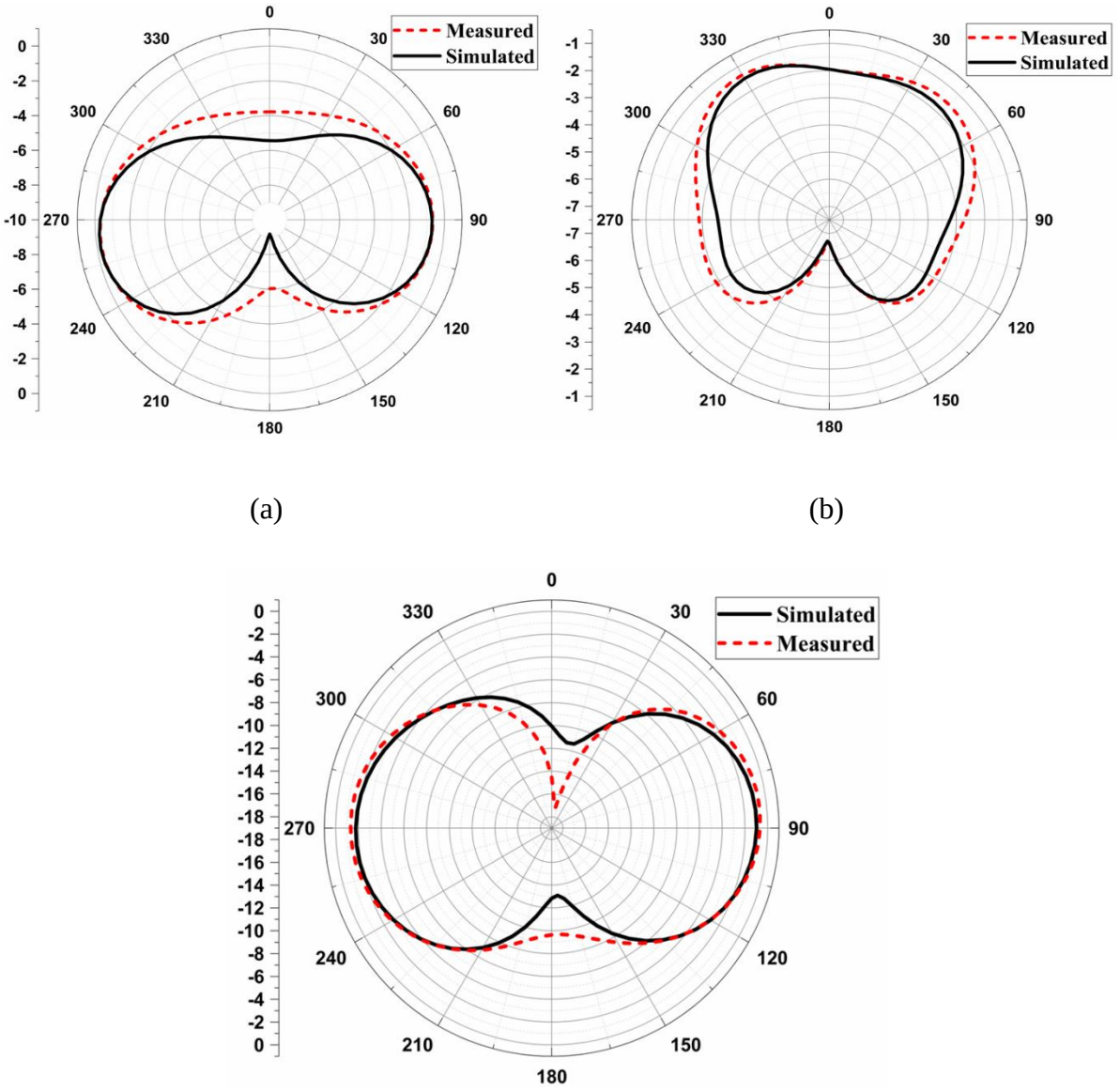

Figure 13. Simulated and measured radiation pattern of a proposed antenna in terms of elevation angle at 7.4 GHz (a) $\theta = 60^{o}$ (b) $\theta = 120^{o}$ (c) $\theta = 180^{o}$.

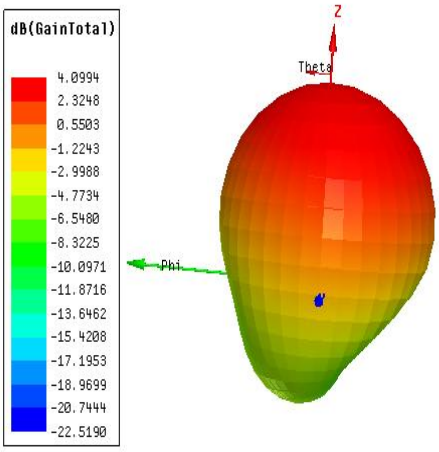

Figure 14. 3D Gain plot of the proposed antenna.

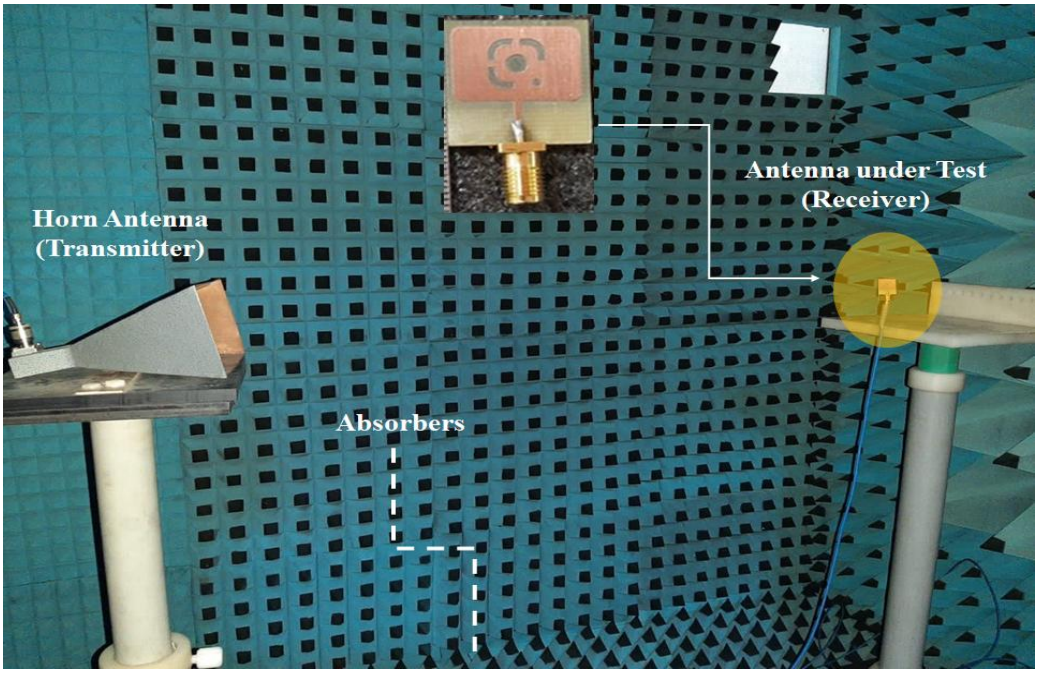

Figure 15. Measurement setup of gain and radiation pattern in an anechoic chamber.

Table 2 compares several antennas that have been previously published in the literature to the proposed broadband antenna for wireless applications. The antenna shown in [17,22] was big and did not shift all the resonant frequencies of wireless applications. When compared to the antenna we constructed, the antenna suggested in [18] offered a modest gain. The antenna in [19] was huge in size and had a constrained impedance bandwidth. The antenna in [20] had a straightforward design, but didn't cover all of the necessary bands for our resonant frequencies and had a lower gain than our antenna. According to [21], the antenna only covered some of the bands and featured a complicated construction printed in Taconic RF-35. The comparison demonstrates that the proposed broadband antenna has a number of benefits over earlier reported antennas [8–22] in terms of size, impedance bandwidth, and gain.

Table 2. Comparison of the suggested antenna performances with other antennas in the literature.

Reference No	Size (mm^2)	Type of Substrate	Bandwidth (GHz)	Resonant Frequency (GHz)	Peak Gain (dB)
[17]	60 ×90	FR-4	0.7 0.3	2.4 5.2 5.6	2.76 2.9 2.44
[18]	57 ×31.2	FR-4	0.3 0.9 0.85	2.45 3.5 5.5	1.19 1.59, 2.39
[19]	56 ×37	FR-4	0.26 0.39 0.2 0.19	2.43 3.83 4.48 5.8	2.2 2.8 3.3 2.2
[20]	60 ×60	FR-4	0.3 0.4	2.46 3.5	2.61 2.7
[21]	120 ×70	Taconic RF-35	1.98	2.46 3.5	2.11 3.48
[22]	60 ×45	FR-4	0.7 0.26	2.6 3.5	3.1 3.3
[23]	50 ×50	FR-4	0.22	3.6 5.3	2.78 2.32
Proposed Work	**20 x 20**	**FR-4**	**0.26** **0.16**	**5.3** **7.4**	4.094 4.094

4. Conclusions

A dual-band google lens logo-based patch antenna with a defected ground structure at 5.3 GHz and 7.4 GHz is designed and fabricated. This antenna is printed on an FR4 substrate with a dimension of 20 × 20 × 1.6 mm^3. Wide impedance bandwidths of 0.23 GHz (5.17–5.40 GHz) and 0.16 GHz (7.33–7.49 GHz) at center frequencies of 5.3 GHz and 7.4 GHz were utilized for wireless applications and WIFI applications, respectively. The return loss characteristics for dual bands are -20.56 dB at 5.3 GHz and -19.17 dB at 7.4 GHz, respectively, with a VSWR < 2 at both the frequencies and a 4 dB gain is obtained. This antenna achieves a considerable peak gain of 4 dB with a radiation efficiency of 61.7% at both resonant frequencies. Moreover, the proposed antenna offers an omnidirectional radiation pattern in both E and H-planes.

Conflict of interest

All authors declare no conflicts of interest in this paper.

References

1. Yoo JU, Son HW (2020) A simple compact wideband microstrip antenna consisting of three staggered patches. *IEEE Antenn Wirel Pr* 19: 2038–2042. https://doi.org/10.1109/LAWP.2020.3021491

2. Babu MR, Venkatachari D, Yogitha K, Sri KP, Jagadeesh K, Lokesh M (2020) A Low-Profile Pentagon Inscribed in Circle Shaped Wide Band Antenna Design for C-Band Applications. *2020 IEEE Bangalore Humanitarian Technology Conference (B-HTC)*, 1–4. IEEE.
3. Chen S, Jiang Y, Cao W (2020) A Compact Ultra-Wideband Microstrip patch Antenna for 5G and WLAN. 2020 IEEE 3rd International Conference on Electronic Information and Communication Technology (ICEICT), 601–603. IEEE. https://doi.org/10.1109/ICEICT51264.2020.9334347
4. Kumar G, Grover K, Kulshrestha S (2019) A Compact Microstrip CP Antenna Using Slots and Defected Ground Structure (DGS). *2019 IEEE Indian Conference on Antennas and Propogation (InCAP)*, 1–4. IEEE. https://doi.org/10.1109/InCAP47789.2019.9134558
5. Patanvariya DG, Kola KS, Chatterjee A (2019) A Circularly-polarized Linear Array of Maple-leaf shaped Antennas for C-band Applications. *2019 10th International Conference on Computing, Communication and Networking Technologies (ICCCNT)*, 1–5. IEEE. https://doi.org/10.1109/ICCCNT45670.2019.8944595
6. Mahatmanto BP, Apriono C (2020) High Gain 4 × 4 Microstrip Rectangular Patch Array Antenna for C-Band Satellite Applications. *2020 FORTEI-International Conference on Electrical Engineering (FORTEI-ICEE)*, 125–129. IEEE. https://doi.org/10.1109/FORTEI-ICEE50915.2020.9249810
7. Maddio S, Pelosi G, Selleri S (2020) A Tri-Band Circularly Polarized Patch Antenna for WiFi Applications in S-and C-band. *2020 IEEE International Symposium on Antennas and Propagation and North American Radio Science Meeting*, 1963–1964. IEEE. https://doi.org/10.1109/IEEECONF35879.2020.9330117
8. Srivastava S, Singh AK (2019) Design of Tri-band L Shaped Parasitic Patch Antenna. *2019 URSI Asia-Pacific Radio Science Conference (AP-RASC)*, 1–4. IEEE. https://doi.org/10.23919/URSIAP-RASC.2019.8738672
9. Abdi M, Aguili T (2019) Design of a Compact Multilayered Aperture Coupled Microstrip Antenna for Automotive Range Radar Application. *2019 IEEE 19th Mediterranean Microwave Symposium (MMS)*, 1–4. IEEE. https://doi.org/10.1109/MMS48040.2019.9157286
10. Xu J, Hong W, Jiang ZH, Zhang H (2018) Wideband, low-profile patch array antenna with corporate stacked microstrip and substrate integrated waveguide feeding structure. *IEEE T Antenn Propag* 67: 1368–1373. https://doi.org/10.1109/TAP.2018.2883561
11. Patanvariya DG, Chatterjee A (2020) A Compact Triple-Band Circularly Polarized Slot Antenna for MIMO System. *2020 International Symposium on Antennas & Propagation (APSYM)*, 54–57. IEEE. https://doi.org/10.1109/APSYM50265.2020.9350733
12. Chen WS, Lin YC, Huang KH (2020) Design of 8-port Cross-Slot Antennas for WRC 5G C-Band MIMO Access Point Applications. *2020 International Workshop on Electromagnetics: Applications and Student Innovation Competition (iWEM)*, 1–2. IEEE. https://doi.org/10.1109/iWEM49354.2020.9237426
13. Sara S, Abdenacer ES (2019) Novel dual-band dipole antenna integrated with EBG electromagnetic bandgap structures dedicated to mobile communications. *2019 International Conference on Wireless Technologies, Embedded and Intelligent Systems (WITS)*, 1–5. IEEE. https://doi.org/10.1109/WITS.2019.8723660
14. Sokunbi O, Gaya S, Hamza A, Sheikh SI, Attia H (2020) Enhanced Isolation of MIMO Slot Antenna Array Employing Modified EBG Structure and Rake-Shaped Slots. *2020 IEEE*

International Symposium on Antennas and Propagation and North American Radio Science Meeting, 1969–1970. IEEE. https://doi.org/10.1109/IEEECONF35879.2020.9329691

15. Sharma GK, Sharma N (2013) Improving the Performance Parameters of Microstrip Patch antenna by using EBG substrate. *IJRET: International Journal of Research in Engineering and Technology* 2: 111–115. https://doi.org/10.15623/ijret.2013.0212019
16. Ghouz HHM, Sree MFA, Ibrahim MA (2020) Novel wideband microstrip monopole antenna designs for WiFi/LTE/WiMax devices. *IEEE Access* 8: 9532–9539. https://doi.org/10.1109/ACCESS.2019.2963644
17. Palandoken M (2017) Dual broadband antenna with compact double ring radiators for IEEE 802.11 ac/b/g/n WLAN communication applications. *Turk J Electr Eng Comput Sci* 25: 1325–1333. https://doi.org/10.3906/elk-1507-121
18. Chu HB, Shirai H (2018) A compact metamaterial quad-band antenna based on asymmetric E-CRLH unit cells. *PIER C* 81: 171–179. https://doi.org/10.2528/PIERC17111605
19. Chouhan S, Panda DK, Kushwah VS, Singhal S (2019) Spider-shaped fractal MIMO antenna for WLAN/WiMAX/WiFi/Bluetooth/C-band applications. *AEU Int J Electron Commun* 110: 152871. https://doi.org/10.1016/j.aeue.2019.152871
20. Ali WAE, Ashraf MI, Salamin MA (2021) A dual-mode double-sided 4 × 4 MIMO slot antenna with distinct isolation for WLAN/WiMAX applications. *Microsyst Technol* 27: 967–983. https://doi.org/10.1007/s00542-020-04984-6
21. Altaf A, Seo M (2020) Dual-Band Circularly Polarized Dielectric Resonator Antenna for WLAN and WiMAX Applications. *Sensors* 20: 1137. https://doi.org/10.3390/s20041137
22. Liu S, Wu W, Fang DG (2015) Single-Feed Dual-Layer Dual-Band E-Shaped and U-Slot Patch Antenna for Wireless Communication Application. *IEEE Antenn Wirel Pr* 15: 468–471. https://doi.org/10.1109/LAWP.2015.2453329
23. Benkhadda O, Ahmad S, Saih M, Chaji K, Reha A, Ghaffar A, et al. (2022) Compact Broadband Antenna with Vicsek Fractal Slots for WLAN and WiMAX Applications. *Appl Sci* 12: 1142. https://doi.org/10.3390/app12031142
24. Kumar A, Raghavan S (2018) Planar Cavity-Backed Self-Diplexing Antenna Using Two-Layered Structure. *Progress In Electromagnetics Research Letters* 76: 91–96. https://doi.org/10.2528/PIERL18031605
25. Kumar A, Imaculate Rosaline S (2021) Hybrid half-mode SIW cavity-backed diplex antenna for on-body transceiver applications. *Appl Phys A* 127: 1–7. https://doi.org/10.1007/s00339-021-04978-9
26. Kumar A, Chaturvedi D, Raghavan S (2019) Design and experimental verification of dual-Fed, self-diplexed cavity-backed slot antenna using HMSIW technique. *IET Microw Antennas Propag* 13: 380–385. https://doi.org/10.1049/iet-map.2018.5327
27. Saravanakumar M, Kumar A, Raghawan S (2019) Substrate Integrated Waveguide-fed Wideband Circularly Polarised Antenna with Parasitic Patches. *Defence Sci J* 69. https://doi.org/10.14429/dsj.69.13049
28. Kumar A, Chaturvedi D, Raghavan S (2019) Dual-Band, Dual-Fed Self-Diplexing Antenna. *2019 13th European Conference on Antennas and Propagation (EuCAP)*, 1–5. IEEE.
29. Imamdi G, Narayana MV, Navya A, Roja A (2018) Reflector array antenna design at millimetric band for on the move applications. *ARPN Journal of Engineering and Applied Sciences* 13: 352–359.

30. Govardhani I, Narayana MV, Navya A, Venkatesh A, Spurjeon SC, Venkat SS, et al. (2017) Design of high directional crossed dipole antenna with metallic sheets for UHF and VHF applications. *International Journal of Engineering & Technology* 7: 42–50. https://doi.org/10.14419/ijet.v7i1.5.9120
31. Narayana MV, Immadi G, Navya A, Anirudh D, Naveen K, Sriram M (2020) A Non- Foster Elemental Triangular Shaped Patch Antenna for Fm Applications. *JCR* 7: 468–470. https://doi.org/10.31838/jcr.07.13.82
32. Immadi G, Narayana MV, Navya A, Anudeep Varma C, Reddy A, Manisai Deepika A, et al. (2020) Analysis of substrate integrated frequency selective surface antenna for IOT applications. *Indonesian Journal of Electrical Engineering and Computer Science* 18: 875–888. https://doi.org/10.11591/ijeecs.v18.i2.pp875-881

AIMS Press